

USING A NEW FAULTED SYNCHRONOUS MACHINE MODEL FOR HARDWARE-IN-LOOP TESTING OF A GENERATOR PROTECTION RELAY

Y-T Huang[#], B S Rigby^{*†}, A B Dehkordi[‡]

University of KwaZulu-Natal[#] etalumiSe (Pty) Ltd^{*} Durban University of Technology[†] RTDS Technologies Inc., Canada[‡]

ABSTRACT

This paper presents the results of a study into the use of a new faulted synchronous generator model for testing generator protection schemes using a real-time simulator. The paper presents results of tests on stator differential, loss of excitation and 100% stator ground fault protection schemes.

INTRODUCTION

Hardware-in-loop testing of relays connected to real-time simulation models of protected plant has become a well-established method of analysis and testing in many sub-disciplines of the field of protection. However, until recently even the most detailed dynamic models of synchronous generators that were available in simulation programs were very limited when it came to the particular requirements demanded by protection studies. Recently though, a new model has recently become available that allows representation of internal winding faults in the stator circuits of a synchronous machine as well as faults in the excitation systems feeding the field circuits of these machines in real-time simulation studies [1,2].

In large synchronous generators, different stator winding protection schemes are recommended in practice depending on the particular grounding method used on the machines [3]. The particular measurement requirements of these different protection schemes, in turn, have implications for the extent to which it may be possible to test their hardware and settings using a real-time simulator.

This paper presents the results of a research study currently being conducted to evaluate the use of this new faulted synchronous machine model for conducting hardware-in-loop testing of a number of protection functions on a practical generator protection relay [4].

STUDY SYSTEM AND METHODS

Fig. 1 shows a schematic diagram of the study system that is being used for this research project. The system comprises four 555 MVA generators at a power station connected to a remote system (represented as an infinite bus) via two transmission lines. This system was chosen for study since it is a well-known benchmark for the study of generator stability [5] and as such has documented parameters that are not only representative of large generators but also of their controllers; the availability of detailed and realistic controller information is important for studies into many aspects of generator protection that are influenced by, and in

turn inter-related with system stability issues. The diagram illustrates that for these studies, all four generator and step-up transformer units in the study system of [5] have been represented explicitly within the real-time model, both to allow connection of a protection relay to the real-time model of a single generator for study (Unit 1), but also to allow further studies into the influence of faults on other generators in the station, and the resulting inter-machine swings, on the protection of the first generator.

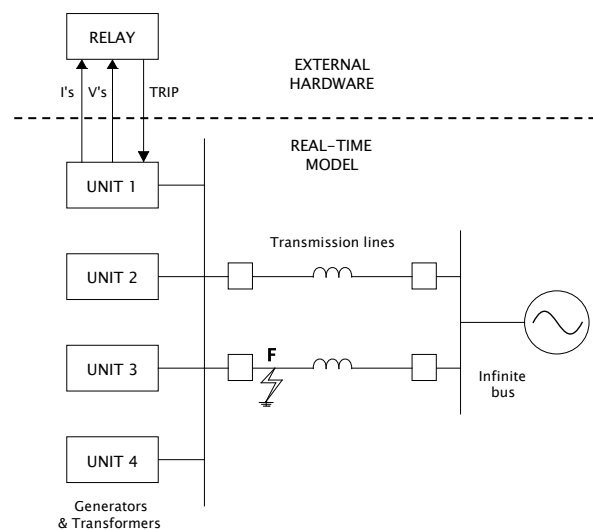


Fig. 1 – Single line diagram of the full study system.

The diagram in Fig. 1 also illustrates how hardware-in-loop studies are carried out on the real-time simulator. All the electrical plant in the power station and the remote system is modelled mathematically on the real-time simulator. For the particular generator and transformer unit whose protection is being studied, instrument transformers are included in the real time model to measure the voltages and currents required by the protection, and the secondary variables from them are exported for injection into the external hardware relay being used to protect the generator. The trip signals from this external relay are then fed back into simulator and used to operate the appropriate circuit breakers within the real-time model of the plant.

The particular relay hardware being used for these studies is a multi-function generator protection relay [4] that had been donated to the research centre where the studies are being conducted. Table 1 shows a summary of some of the elements available on this relay, but the particular elements focused on in this paper are the loss of field (LOF) protection (40), and two distinct types of stator protection, 100% stator ground fault protection (64G) and phase percentage restrained differential

protection (87P). The 87P element can be used for stator winding protection on generators that employ low-impedance grounding [3,4]. The first part of this paper therefore focuses on the use of this particular form of stator protection and its analysis using real-time simulator models.

Table 1 – Generator protection relay elements

Device	Description
21	Backup distance protection
24	Volts per Hertz protection
25	Synchronism checking
27	Undervoltage element
32	Reverse/Low-forward power protection
40	Loss-of-field protection
46	Negative sequence overcurrent protection
50P/N	Phase and neutral overcurrent protection
51	Voltage restrained time-overcurrent protection
59	Overvoltage element
60	Loss-of-potential protection
64G	100% stator ground fault protection
78	Out-of-step protection
81	Frequency protection
87P	Phase percentage restrained differential protection
AE	Inadvertent energization protection

Fig. 2 shows a subset of the real-time simulation model implementation of the full study system in Fig. 1 highlighting just those parts of the model that are associated with the particular unit whose protection was the subject of study (Unit 1). On the left-hand side of Fig. 2 is the component model of the synchronous generator which, by representing all the generator windings in the phase domain [1,2] allows phase-to-

ground faults to be applied at user-specified variable locations along the stator winding during the simulation as shown. Fig. 2 shows that this new form of machine model now also allows the excitation system of the generator to be modelled realistically as an explicit electrical circuit that forms part of the electromagnetic transients solution, rather than simply as a control-signal type of input to the machine model; consequently, the model is therefore able to include a detailed representation of the generator’s field breaker that can be opened and closed while the simulation runs, and user-controlled short-circuit faults can likewise be applied in the field circuit during the run.

When studying the performance of the 87P element of the relay, the generator was grounded through a low resistance, and the generator neutral breaker and its controls, and the earthing resistor itself were all included in the real-time simulation model as shown in Fig. 2. The 87P element of the relay can be used to cover just the generator stator windings or it can include the windings of the generator transformer [4]; the real-time model was therefore configured to allow application of internal winding faults at specified locations in all three phases of the transformer as well as faults in between the generator and transformer to allow the performance of the 87P element to be assessed in both of these application modes. The generator’s main (AC) circuit breaker was also represented in the real-time model and controlled by the external relay hardware.

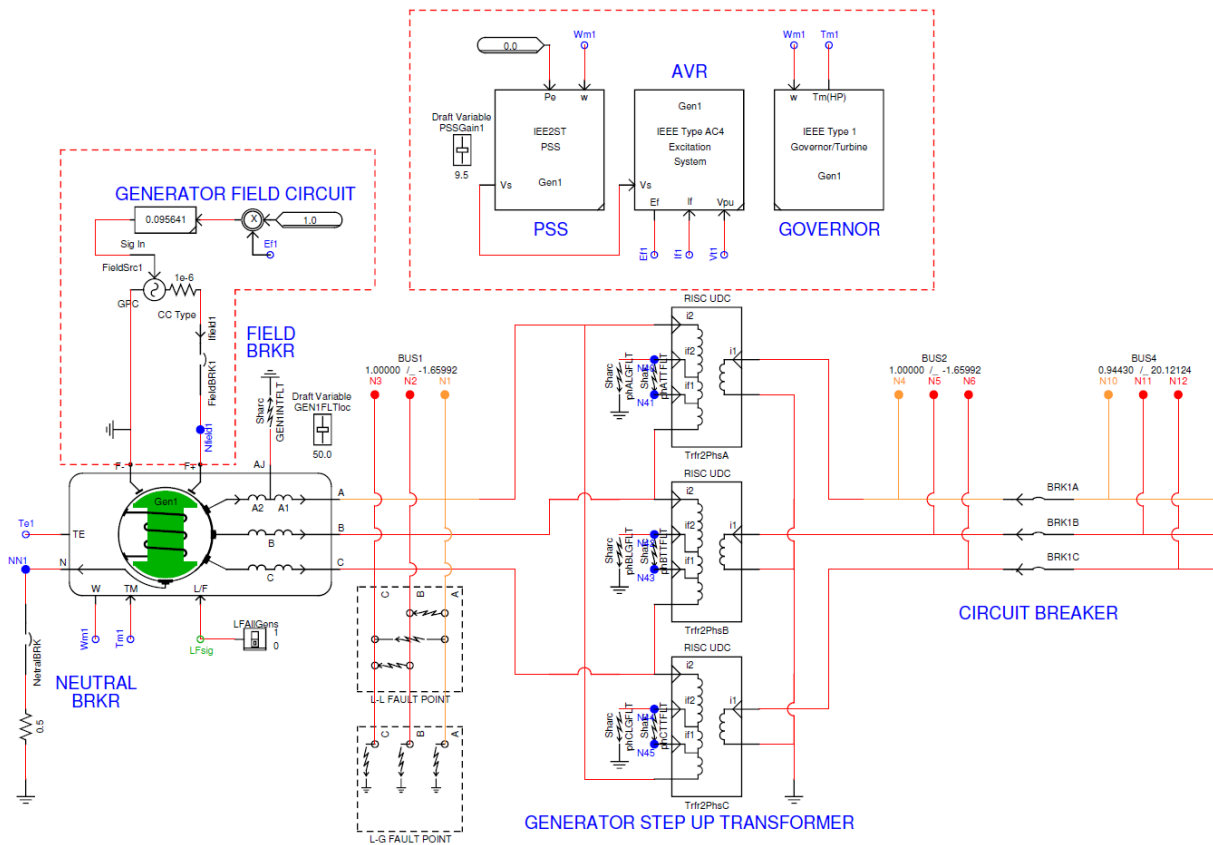


Fig. 2 – Real-time modelling details of one generator in the study system for low-impedance grounding protection tests.

The measured variables from the generator that need to be exported to the external relay depend on what particular protection functions are being studied in the relay. For this first case considered in the tests (low-impedance grounded generator) the currents were measured at both ends (neutral and terminal) in all three phases of the generator windings and exported to the relay for its 87P elements as well as the stator terminal voltages in all three phases as required for the LOF (40) element. (For simplicity, the instrument transformers actually used in the model are not shown in Fig. 2).

RESULTS: LOW IMPEDANCE GROUNDED GENERATOR

The protection relay being used in the tests was connected hardware-in-loop with one of the four generators in the real-time model of the study system for the low-impedance grounding case example shown in Fig. 2. A range of faults were applied to test both the stator differential protection (87P), and loss-of-field protection (40) elements of the relay.

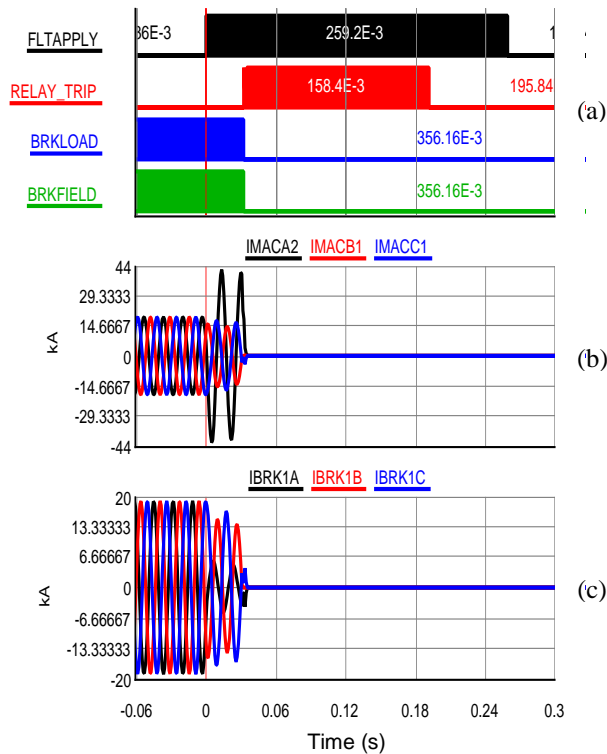


Fig. 3 – Real-time simulation variables for stator ground fault at 95%: (a) binary control signals; (b) winding currents at neutral end; (c) winding currents at stator terminal end.

Stator Differential Protection (87P)

A phase-to-ground fault was applied from the node AJ of the stator winding in the faulted generator model of Fig. 2 with the location of the fault set at 95% along the winding from the neutral end. Fig. 3(a) shows the response of the relay's trip signal and the opening of the circuit breakers in the real-time model of the plant following the application of this fault. Figs. 3(b) and (c) show the instantaneous phase currents measured at both ends of the generator windings for this fault test. When

the fault is applied, there is a significant difference in the current measured at each end of the winding in the faulted phase. The 87P element of the relay detects this difference and interrupts all three phase currents by issuing a trip.

Figs. 4(a) and (b) show the operating and restraint currents versus time for the faulted phase (phase A) and one healthy phase (phase B) as seen by the event recorder of the external relay for this same fault test. As expected, a large operating current is seen in the faulted phase but not in the healthy phase.

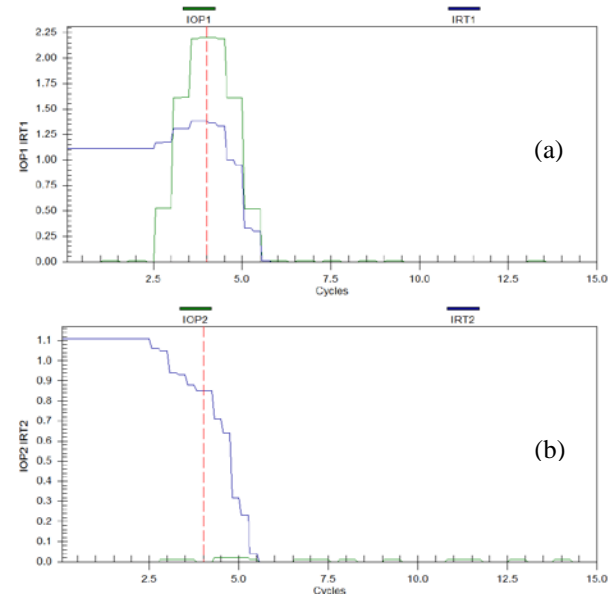


Fig. 4 – Operating and restraint currents versus time recorded by the hardware relay's event recorder for the ground fault located at 95%: (a) faulted phase A; (b) healthy phase B.

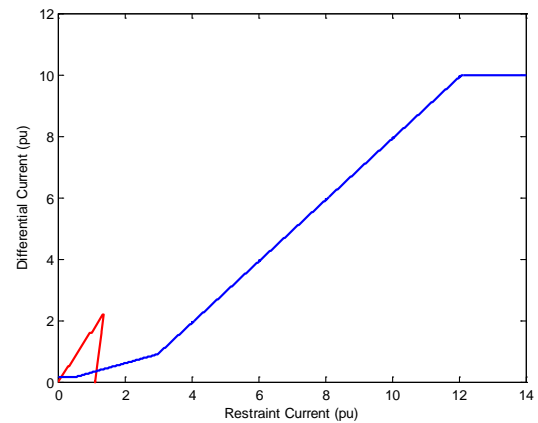


Fig. 5 – Operating current versus restraint current for faulted phase A overlaid onto the differential characteristic of the relay; fault at 95% along the winding.

Figs. 5 and 6 show the operating and restraint currents for the faulted phase plotted against one another – and overlaid onto the differential characteristic that was set in the 87P element of the relay – for two different locations of the fault along the winding, namely at 95% and at 10%. As already seen in Fig. 3, the relay successfully issued a trip signal to clear the ground fault located at 95% along the stator winding; Fig. 5

illustrates that this is because there was sufficient operating current to cause the operating versus restraint current trajectory to pass into the tripping area of the relay's differential characteristic.

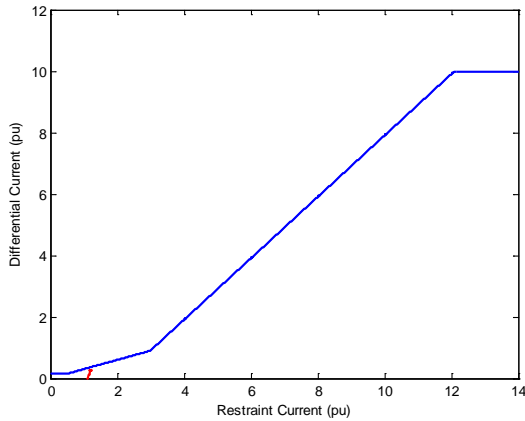


Fig. 6 – Operating current versus restraint current for faulted phase A overlaid onto the differential characteristic of the relay; fault at 10% along the winding.

By contrast, the 87P element of the relay did not trip for the ground fault located at 10% along the stator winding. The magnitude of the current in a ground fault becomes progressively smaller as the fault moves closer to the neutral end of the stator winding. Fig. 6 illustrates that for the fault at 10% there was insufficient operating current to cause the operating versus restraint current trajectory to pass into the tripping area of the differential characteristic.

It is expected that differential protection is not able to detect faults close to the neutral end of the winding [4]. Tests such as those shown above were therefore repeated for a range of fault positions along the stator winding to determine the extent to which the 87P element could cover the stator winding for ground faults in this particular application. The results of these tests, summarised in Table 2, show that, in this instance, the phase differential protection could not detect ground faults in the bottom 13% of the stator winding.

Table 2 – Stator differential protection coverage

FLT LOC (%)	Relay response
0	No trip
5	No trip
6	No trip
7	No trip
8	No trip
9	No trip
10	No trip
11	No trip
12	No trip
13	No trip
14	Tripped
15	Tripped
⋮	⋮
50	Tripped
55	Tripped
⋮	⋮
95	Tripped
100	Tripped

Loss Of Field Protection (40)

When a generator loses excitation (field current), it consumes a large amount of reactive power from the external power system in order to support its terminal voltage. However, this excessive reactive power intake will cause damage to the generator and also threaten the stability of the system. Therefore the loss-of-field protection is intended to detect conditions when the excitation is below the minimum excitation limit. In practice, complete loss of excitation could occur in two ways: a short circuit fault in the excitation system, or an open circuit condition caused by inadvertent opening of the field breaker. The real-time simulation model of the low-impedance grounded generator in Fig. 2 was used to investigate the response of the generator protection relay to each of these scenarios.

Excitation System Short Circuit. The real-time model was used to apply a short circuit fault between one terminal of the generator field circuit and ground, and the response of the generator and its protection scheme was recorded. When the short circuit occurred in the excitation system, the generator terminal voltage started to decrease and the stator current started to increase as shown in the results of Figs. 7(b) and (c) respectively. As the magnetic coupling between the generator and the system became weakened due to the loss-of-field, the generator would have eventually pole-slipped had no action been taken. However, as shown in Fig. 7(a), the relay issued a trip approximately 3.5 seconds after the field short circuit occurred.

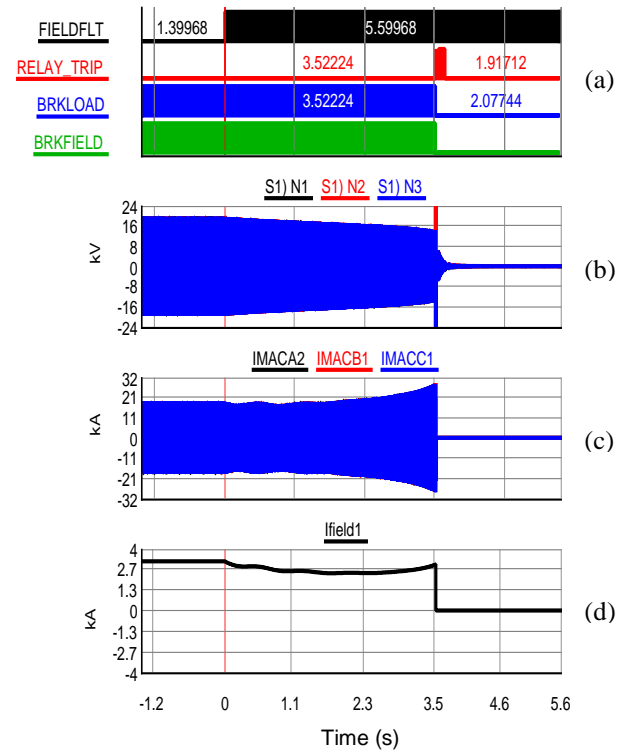


Fig. 7 – Real-time simulation variables for field short circuit test: (a) binary control signals; (b) generator stator voltages; (c) generator stator currents; (d) generator field current.

The relay's response to this fault can be understood by examining the impedance seen by the relay, overlaid onto the settings characteristics of its LOF element as chosen for this generator, as shown in Fig. 11. The results in Fig. 11 show that the impedance locus took 3.523 seconds before it encroached the inner mho circle. This inner mho circle of the LOF protection was set to have no intentional time delay, whilst the time delay for the outer mho circle was set to 0.5 seconds in order to avoid mis-operation for the worst-case stable swing of the generator.

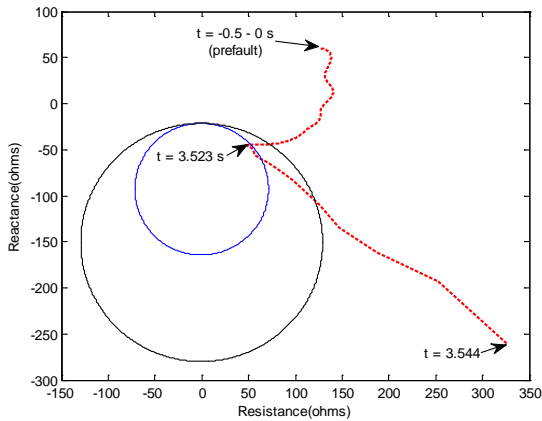


Fig. 8 – Impedance locus overlaid onto the relay's loss-of-field element's operating characteristics for the excitation system short circuit test.

Inadvertent Open Circuiting Of The Field. The real-time model was used to study the response of the protection to an inadvertent open circuiting of the field by opening the field circuit breaker during normal operation of the generator. The generator terminal voltages and stator currents were subjected to an abrupt change following this loss of field current as can be seen from Figs. 9(b) and (c).

Fig. 10 shows that for the open circuit loss of excitation condition, the impedance locus seen by the relay encroached into the outer mho circle first, but the relay did not issue a trip since there was a 0.5 s time delay set for this zone. The relay only tripped after the impedance locus had encroached into the inner mho circle at time $t = 0.56$ seconds as shown in Fig. 10.

Consequences Of Breaker Failure

An important practical consideration in low-impedance grounded generators is the fact that the fault currents do not stop flowing when the generator is tripped from the system and its field is disconnected: fault currents can continue to flow for several seconds because of trapped flux within the machine, increasing the possibility of damage to plant. Consequently, in these generators, not only is high-speed protection essential but it is desirable to operate a breaker in the generator neutral circuit as well in order to de-energise the machine as quickly as possible. The fact that the faulted phase-domain synchronous generator model in the real-time simulation

environment is able to represent the generator field winding properly, as an electrical circuit rather than as an input set by a control-type variable, means that this model can be used to study the practical implications of different fault clearing actions in the generator and the impact of failure of one or more breakers to operate.

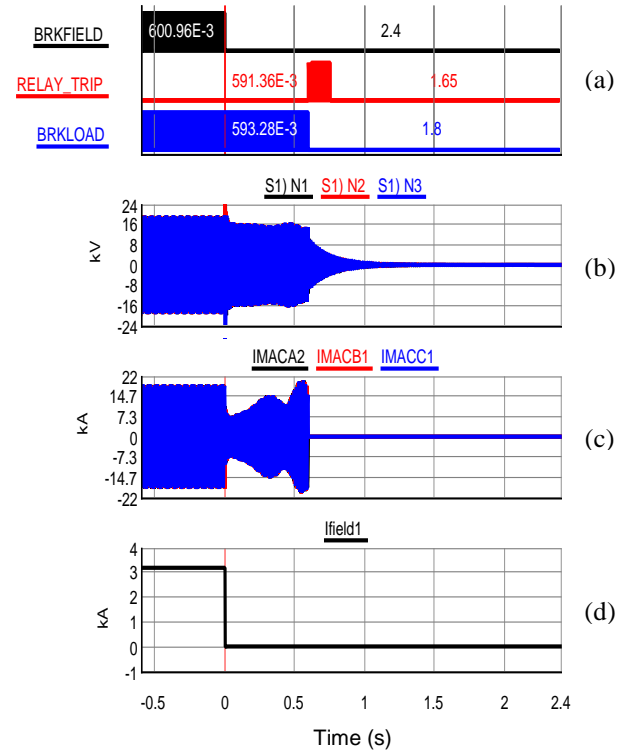


Fig. 9 – Real-time simulation variables for field open circuit test: (a) binary control signals; (b) generator stator voltages; (c) generator stator currents; (d) generator field current.

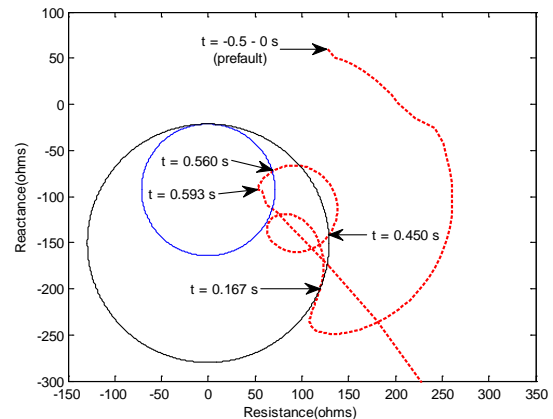


Fig. 10 – Impedance locus overlaid onto the relay's loss-of-field element's operating characteristics for the excitation system open circuit test.

As an example, Fig. 11 shows the results obtained from the real-time simulation model when the 87P element of the relay issued a trip in order to clear a ground fault in one phase of the stator winding of the low-impedance grounded generator, but where only the stator terminal breaker was opened in response to this trip signal. The

results show that opening the stator terminal breaker on its own only interrupts the current being fed into the ground fault in the affected phase from that side of the stator winding, whilst substantial current (tens of kiloamps) continues to flow into the fault from the neutral-end of the winding as the field current continues to energise the bottom section of the winding in the faulted phase.

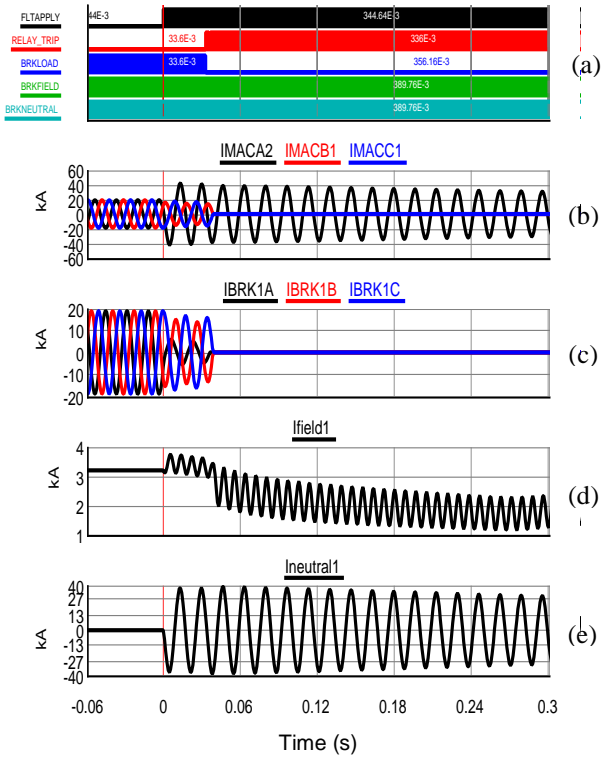


Fig. 11 – Simulation of stator winding fault cleared by opening only the main breaker: (a) binary control signals; (b) winding currents at neutral end; (c) winding currents at stator terminal end; (d) generator field current; (e) generator neutral current.

By comparison, Fig. 12 shows the results when the same fault is cleared by opening both the stator terminal breaker and the field breaker, but with the neutral breaker remaining closed. In this case, the removal of the field current is able to reduce the energisation of the faulted winding, although not completely, and the result is a reduced amplitude of current in the bottom part of the faulted winding that decays faster, but which is still on the order of tens of kiloamps and persists for several hundred milliseconds after the breakers are opened.

Finally, Fig. 13 shows that opening all three breakers in response to the relay trip signal (stator, field and neutral) rapidly reduces the fault current and the potential for damage.

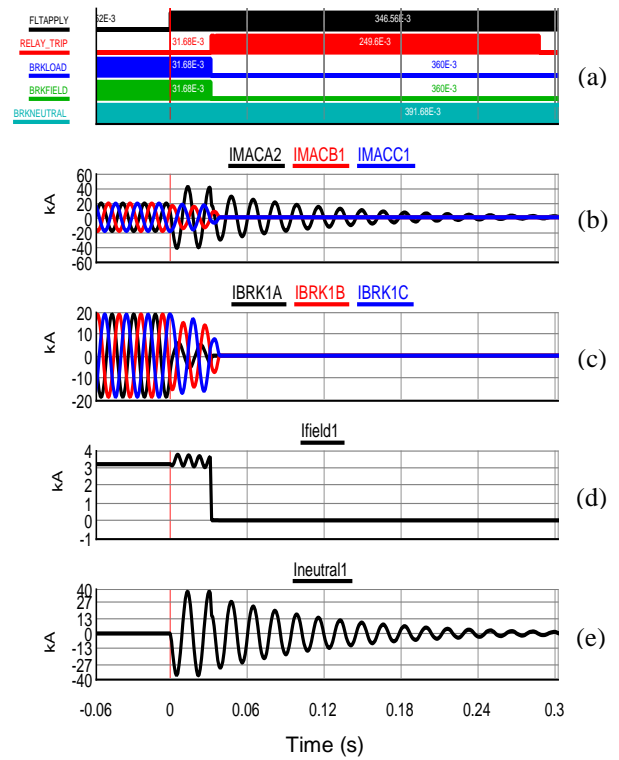


Fig. 12 – Simulation of stator winding fault cleared by opening main and field breakers: (a) binary control signals; (b) winding currents at neutral end; (c) winding currents at stator terminal end; (d) generator field current; (e) generator neutral current.

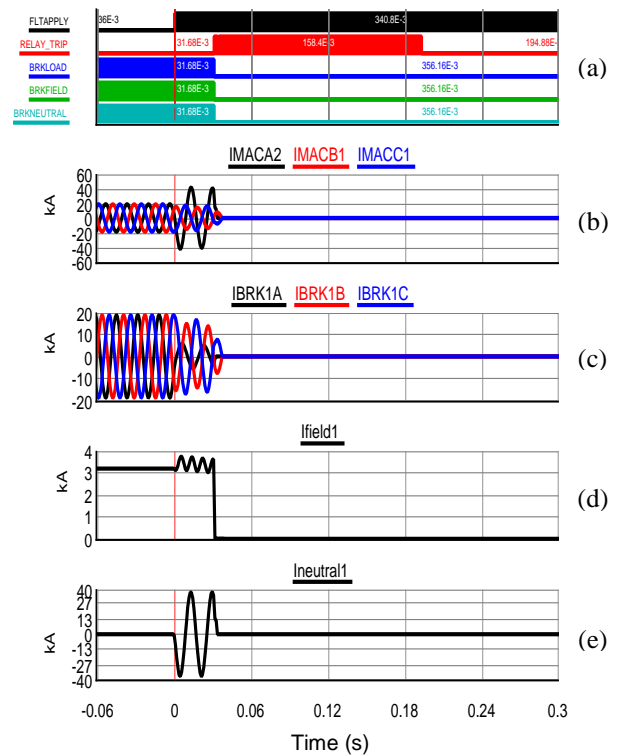


Fig. 13 – Simulation of stator winding fault cleared by opening main, field and neutral breakers: (a) binary control signals; (b) winding currents at neutral end; (c) winding currents at stator terminal end; (d) generator field current; (e) generator neutral current.

The bottom part of Fig. 14 is an additional circuit that was included within the real-time model to represent the behaviour of the generator's third-harmonic winding voltages (and their relative magnitudes at the neutral and stator terminals of the generator) under both unfaulted and faulted conditions. The dynamically-controlled voltage sources in each phase of this equivalent circuit representation were programmed to replicate the specific characteristics of actual third-harmonic winding voltages (including their dependence on generator loading) of a comparably-rated large synchronous generator reported in [7]. The modelling elements used to program these equivalent-circuit voltage sources so as to replicate this generator's load-dependent third-harmonic voltage behaviour (or that of any other machine of interest) are shown here in the separate diagram of Fig. 15.

The phase-domain faulted synchronous generator model and the custom-designed third-harmonic equivalent circuit model are simulated together in the same real-time simulation case and their output voltages added together to provide the total voltages (fundamental plus third harmonic) sent to the external relay being tested.

RESULTS: 100% STATOR GROUND FAULT PROTECTION (64G)

Hardware-in-loop connection of a practical relay with the real-time simulation model of the high-resistance grounded generator case example shown in Figs. 14 and 15 was used to assess whether this modelling approach was suitable for testing a 100% stator ground fault protection scheme. On the particular relay being used [4] the fundamental-frequency neutral overvoltage element (64G1) of the 100% stator ground protection scheme should provide coverage of approximately 95% of the stator winding, but is expected to be unable to detect faults in the bottom 5% of the winding closest to the neutral terminal. By contrast, the third-harmonic differential element (64G2) of the scheme is expected to be able to detect ground faults located at the neutral terminal itself, and upwards from this terminal well into the stator winding, but it is expected to exhibit a lack of coverage over some internal portion of the winding; the extent of this blind region in the 64G2 element's coverage is expected to be dependent on generator loading, but the whole stator winding should be covered by one or both of the two elements that make up the scheme under all conditions (that is, the blind region within each element's coverage should always be complemented by the ability of the other element in the protection scheme to cover that part of the winding).

Ground faults were therefore applied at locations along the entire length of one phase of the stator winding using the model shown in Figs. 14 and 15 at two different generator loading conditions, and the coverage of each element of the relay's 100% stator ground fault protection documented; the results are shown in Tables 3 and 4. These tables confirm that the third-harmonic

differential element, as expected, exhibits a lack of coverage in the middle part of the winding in this case, and that this gap in coverage is larger under no-load conditions than at full load; however, in both cases it provides coverage of the bottom 5% of the winding in the region where the fundamental-frequency neutral overvoltage element cannot detect faults. The measured results in Tables 3 and 4 confirmed that the two complementary elements within the protection scheme did in fact provide coverage of the entire stator winding for ground faults.

Table 3 – Response of hardware relay's 100% stator ground protection elements at no load.

FLT LOC	ELEMENTS	
	64G1	64G2
%	Tripped	Tripped
100	Tripped	Tripped
95	Tripped	Tripped
⋮	⋮	⋮
59	Tripped	Tripped
58	Tripped	No trip
57	Tripped	No trip
56	Tripped	No trip
55	Tripped	No trip
54	Tripped	No trip
53	Tripped	No trip
52	Tripped	No trip
51	Tripped	No trip
50	Tripped	No trip
49	Tripped	No trip
48	Tripped	No trip
47	Tripped	No trip
46	Tripped	No trip
45	Tripped	No trip
44	Tripped	Tripped
⋮	⋮	⋮
5	Tripped	Tripped
0	No trip	Tripped

Table 4 – Response of hardware relay's 100% stator ground protection elements at full load.

FLT LOC	ELEMENTS	
	64G1	64G2
%	Tripped	Tripped
100	Tripped	Tripped
95	Tripped	Tripped
⋮	⋮	⋮
59	Tripped	Tripped
58	Tripped	Tripped
57	Tripped	Tripped
56	Tripped	Tripped
55	Tripped	Tripped
54	Tripped	No trip
53	Tripped	No trip
52	Tripped	No trip
51	Tripped	No trip
50	Tripped	No trip
49	Tripped	Tripped
48	Tripped	Tripped
47	Tripped	Tripped
46	Tripped	Tripped
45	Tripped	Tripped
44	Tripped	Tripped
⋮	⋮	⋮
5	Tripped	Tripped
0	No trip	Tripped

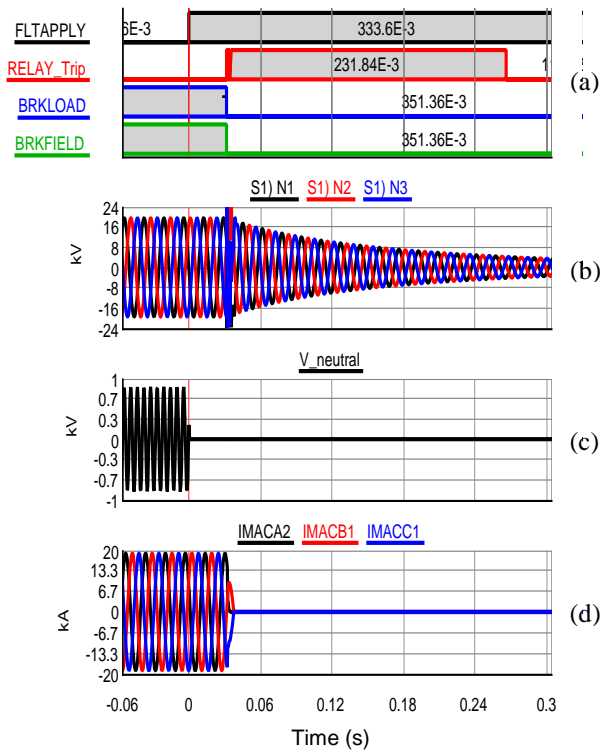


Fig. 16 – Real-time simulation variables for ground fault at the generator neutral: (a) binary control signals; (b) generator stator voltages; (c) generator neutral voltage; (d) generator stator currents.

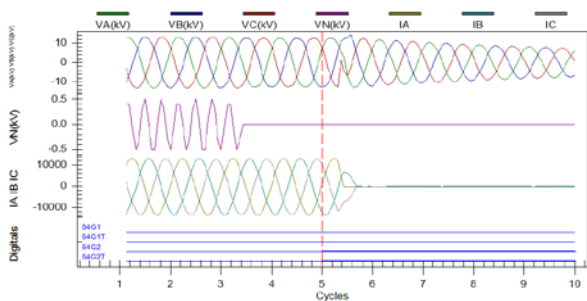


Fig. 17 – Variables recorded by the hardware relay's event recorder for the fault at the generator neutral.

To analyse the characteristics and coverage of the 100% stator ground protection further, detailed results were recorded for faults located in each of the parts of the stator winding not covered by one or other of its two complementary elements. Fig. 16 shows the results from the real-time simulator study for a fault located at the generator neutral terminal. Fig. 16(c) illustrates that under healthy conditions prior to the application of the fault, the generator neutral voltage consists predominantly of third-harmonic frequency, with very little fundamental-frequency component present. However, when the fault is applied at the generator neutral the voltage at this point drops to zero, so that the fundamental-frequency overvoltage element is naturally unable to pick up for this location of fault. However, because the 64G2 element responds to changes in the *relative* third-harmonic voltage magnitudes at either end

of the winding, this element is still able to detect faults right at, or near the neutral despite the fact that the voltage measured at the neutral disappears for faults in this location.

The variables recorded by the external relay hardware's event recorder for this fault, shown in Fig. 17, confirm that the 64G2 element of the relay detected this fault and was responsible for issuing the trip signal input to the real-time simulation model recorded in Fig. 16(a).

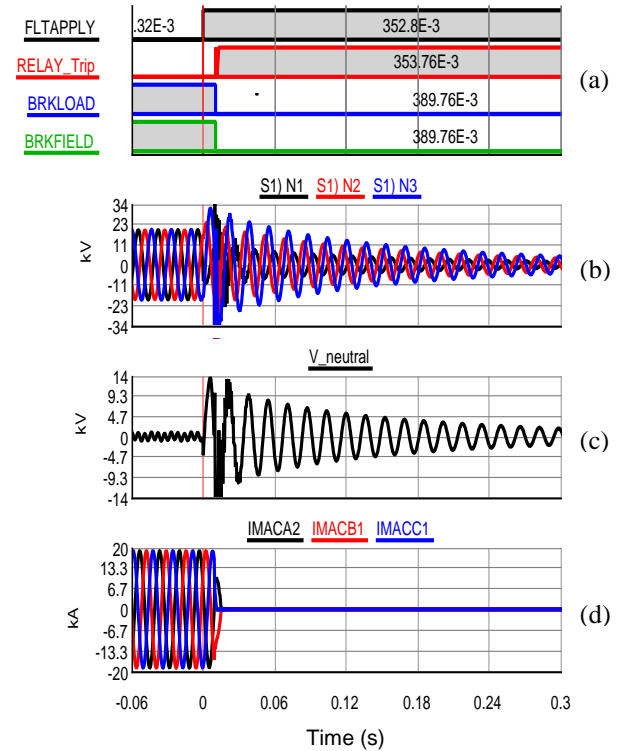


Fig. 18 – Real-time simulation variables for ground fault at 53% along the stator winding: (a) binary control signals; (b) generator stator voltages; (c) generator neutral voltage; (d) generator stator currents.

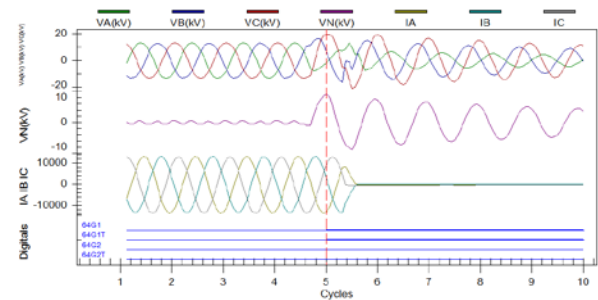


Fig. 19 – Variables recorded by the hardware relay's event recorder for the fault at 53% along the stator winding.

Fig. 18 shows the results for a fault applied at 53% along the stator winding from its neutral terminal. For a ground fault at this location in the winding there is almost no detectable change in the third harmonic voltages measured at the ends of the winding (physically, this is because the magnitude profile of the third-harmonic voltage induced in the stator winding

passes naturally through zero at this point in the winding, so shorting the winding to ground at this location has no effect on the terminal voltages at this third-harmonic frequency). However, Fig. 18(c) clearly shows a significant increase in the fundamental-frequency component of the neutral voltage for a ground fault applied in this inner part of the stator winding. The variables recorded by the external relay hardware's event recorder, shown in Fig. 19, confirm that the trip issued in this case was as a result of the operation of the 64G1 fundamental-frequency neutral overvoltage element as expected.

CONCLUSION

Protection of large synchronous generators is a complex discipline that is of critical importance given the capital cost and strategic importance of the equipment being protected. This paper has presented results from a study to evaluate the use of a new phase-domain model of a synchronous generator that allows realistic hardware-in-loop testing of generator protection relays on a real-time simulator.

The results have demonstrated that the model can be used directly to test the performance of generator stator current differential protection schemes. The results have also demonstrated how, as a result of the improved representation of the field winding in this phase-domain machine model, it is possible to study in detail the response of generator protection schemes to faults in the excitation system as well as to study important practical issues such as the procedures for de-energising the generator windings when clearing stator winding faults.

Finally, the paper has also shown a method of using an equivalent-circuit model in conjunction with the phase-domain model of the generator in order to include the characteristics of stator winding third-harmonic voltages as needed for testing third-harmonic differential protection schemes.

REFERENCES

- [1] A.B. Dehkordi, P. Neti, A.M. Gole, T.L. Maguire, "Development and Validation of a Comprehensive Synchronous Machine Model for a Real-Time Environment", *IEEE Transactions on Energy Conversion*, Vol. 25, No. 1, March 2010, pp. 34 – 48.
- [2] A.B. Dehkordi, D.S. Ouellette, P.A. Forsyth, "Protection Testing of a 100% Stator Ground Fault Scheme Using a Phase Domain Synchronous Machine Model in Real-Time", 10th International Conference on Developments in Power System Protection (DPSP 2010), Manchester, UK, March-April 2010.
- [3] IEEE Guide for Generator Ground Protection, IEEE Standard C37.101-1993, April 1994.
- [4] SEL-300G Multifunction Generator Relay Instruction Manual, Schweitzer Engineering Laboratories, Inc., 2007.
- [5] Kundur P, *Power System Stability and Control*, McGraw-Hill Inc., New York, 1994.
- [6] C.H. Griffin, J.W. Pope, "Generator Ground Fault Protection Using Overcurrent Overvoltage and Undervoltage Relays", *IEEE Transactions on Power Apparatus and Systems*, Vol. PAS-101, No. 12, December 1982, pp. 4490 – 4501.
- [7] R.J. Marttila, "Design Principles Of A New Generator Stator Ground Relay For 100% Coverage Of The Stator Winding", *IEEE Transactions on Power Delivery*, Vol. PWRD-1, No. 4, Oct. 1986, pp. 41 – 51.